Angular correlation in He and He-like atomic ions: A manifestation of the genuine and conjugate Fermi holes

Tokuei Sako[*]
Laboratory of Physics, College of Science and Technology, Nihon University, 7-24-1 Narashinodai, Funabashi, 274-8501 Chiba, Japan

Josef Paldus[†]
Department of Applied Mathematics, University of Waterloo, Waterloo, Ontario, Canada N2L 3G1

Geerd H. F. Diercksen[‡]
Max-Planck-Institut für Astrophysik, Karl-Schwarzschild-Strasse 1, D-85741 Garching, Germany
(Received 1 February 2014; published 3 June 2014)

The ground and low-lying singly excited states of the two-dimensional He and He-like atomic ions have been studied by the full configuration interaction method focusing on the angular correlation between the two electrons involved. For small values of the nuclear charge Z_n, the two-electron angular-density distribution for the ground state strongly depends on the two-electron angle ϕ_- reaching a peak at $\phi_- = 0$. This strong dependence on ϕ_- strongly decreases with increasing Z_n along with the decreasing electron-electron interaction. In contrast, the probability-density distribution for the singlet-triplet pair of states of the $(1s)(2p)$ configuration becomes appreciable with increasing Z_n, reaching peaks at $\phi_- = 0$ and at $\phi_- = \pm\pi/2$ for the singlet and triplet states, respectively. This indicates a preference of the two electrons to be on the same side of the nucleus for the singlet $(1s)(2p)\ ^1P$ state and on opposite sides of the nucleus for the triplet $(1s)(2p)\ ^3P$ state. The origin of these angular dependences is rationalized on the basis of the genuine and conjugate Fermi hole concepts.

DOI: 10.1103/PhysRevA.89.062501 PACS number(s): 31.10.+z, 31.15.A−, 32.10.−f

I. INTRODUCTION

The helium atom represents the simplest fundamental system for the exploration of electron correlation effects. It has been extensively studied by both theoreticians and experimentalists. A strong electron correlation in doubly excited states of He and He-like atomic ions (referred to hereafter as He-like systems) has been actively studied ever since the experimental observations of autoionizing levels of He [1,2]. Herrick and Kellman provided a supermultiplet classification of the intrashell doubly excited states of He-like systems based on approximate O(4) symmetry and the analogy with rovibrational levels of a linear triatomic molecule with the two electrons undertaking a triatomic molecular motion with the nucleus at their center [3–5]. This interpretation was consistent with conditional probabilities [6,7] obtained from accurate wave functions by Berry's group, and the Kellman-Herrick model of collective rotational and bending motions of electrons was later confirmed by accurate results for conditional probability densities [8]. Berry's group also studied the helium-isoelectronic series and showed that the collective behavior of electrons becomes less appreciable with the increasing nuclear charge [9]. In the case of *singly* excited states of He-like systems, the correlation energy is much smaller than in the doubly excited states since the former involve a tight $1s$ electron and a diffuse outer electron. In view of the lesser role of the correlation energy, it might seem that the singly excited states of He-like systems are of lesser interest than the doubly excited ones. Yet, there still remains an unsolved and interesting problem in the singly excited states with respect to their angular correlation, which we address in this paper.

The angular correlation in singly excited states of He-like systems has been thoroughly studied by Boyd, Moiseyev, Katriel, Thakkar, and others [10–17], focusing in particular on the understanding of the origin of the first Hund rule [18–24]. These pioneering studies have revealed that (i) the correlation energy $\Delta E_{\rm corr}$ moderately increases with increasing nuclear charge Z_n, (ii) in the singly excited states of He-like systems, the angular correlation dominates the radial correlation [12], and (iii) for the singlet-triplet pair of states of the $(1s)(2s)$ configuration, the dependence of the probability-density distribution on the interelectronic angle is very weak, while for the $(1s)(2p)$ configuration, it becomes appreciable and increases with Z_n [13].

As implied by result (i) listed above, the effective correlation energy for atomic systems as defined by the correlation energy scaled by Z_n^2, namely, $\frac{\Delta E_{\rm corr}}{Z_n^2}$, approaches zero as $Z_n \to \infty$. For increasing Z_n, the wave function of singly excited states of He-like systems should approach, therefore, the wave function of the *independent particle model* (IPM) based on the Hartree-Fock approximation. This should then result in an isotropic probability-density distribution that is independent of the interelectronic angle since there should be little angular correlation between the two electrons according to the IPM.

Contrary to this conclusion, result (iii) by Thakkar and Smith [13] considering the so-called angular correlation coefficients implies that the probability-density distribution for the $(1s)(2p)$ singlet-triplet pair of states for larger Z_n becomes strongly dependent on the interelectronic angle, in spite of the fact that in the $Z_n \to \infty$ limit the electron correlation vanishes.

[*]sako@phys.ge.cst.nihon-u.ac.jp; http://www.phys.ge.cst.nihon-u.ac.jp/~sako/
[†]paldus@uwaterloo.ca; http://www.math.uwaterloo.ca/~paldus/
[‡]ghd@mpa-garching.mpg.de; http://www.mpa-garching.mpg.de/mol_physics/index.shtml

In order to elucidate the origin of this controversy, i.e., the strong dependence of the probability-density distribution for the $(1s)(2p)$ singlet-triplet pair of states in the $Z_n \to \infty$ limit, we examine in the present study the details of the nodal structure of the relevant wave functions in the internal space of a two-dimensional model of the studied systems. We also examine the physical nature of the IPM, as represented by a single-determinant Hartree-Fock wave function, with respect to the angular correlation.

The paper is organized as follows: Sec. II describes our theoretical model and computation methodology. Section III presents our results and their discussion. Section III A starts with the results for the ground state that show a "normal" behavior for the Z_n dependence of angular correlation, i.e., a larger angular correlation for smaller nuclear charges. Section III B presents the results for the singly excited $(1s)(2s)$ and $(1s)(2p)$ singlet-triplet pair of states displaying a counterintuitive trend in the Z_n dependence of angular correlation, namely, a larger angular correlation for larger nuclear charges, when the wave function of the system approaches the IPM wave function. Section III C introduces the concepts of the so-called genuine and conjugate Fermi holes in the internal space, and Sec. III D rationalizes the observed Z_n dependences for the singly excited states in a unified way on the basis of the Fermi and conjugate Fermi holes concept. Section IV then summarizes all of the results of the present study and points out an observability of the strange angular correlation for the $(1s)(2p)$ configuration as observed in actual experiments.

II. THEORETICAL MODEL AND COMPUTATIONAL METHOD

In the present study, the spatial degrees of freedom of each of the two electrons in the helium atom are confined to a two-dimensional xy plane. In the case of the three-dimensional helium atom, this xy plane, as defined by the position of the two electrons and the nucleus, can freely rotate about the three principal axes of inertia by the Euler angles (α, β, γ). In the two-dimensional helium atom, this rotation is limited to the axis normal to the xy plane. Although this two-dimensional (2D) helium atom represents a simplified model, it has all of the characteristic features of the energy spectrum of the three-dimensional helium atom, as was shown in our previous studies [23,24]. This similarity in the energy-level structure of the 2D and 3D helium atom is due to the fact that the dimension of the internal space, given by the internal degrees of freedom of the electrons as defined below, is 3 in either case. This coincidence happens only for two-electron systems so that the following reasoning that is based on a 2D model may not be appropriate for systems involving more than two electrons. By reducing the number of degrees of freedom, the internal part of the wave functions can be easily visualized, permitting us to draw unambiguous conclusions concerning the nature of the angular correlation.

The electronic Hamiltonian for two-dimensional heliumlike systems, $\mathcal{H}_Z$, has the following form:

$$\mathcal{H}_Z/Z_n^2 = -\frac{1}{2}\sum_{i=1}^{2}\nabla_{s,i}^2 - \sum_{i=1}^{2}\frac{1}{|\vec{s}_i|} + \frac{1}{Z_n}\frac{1}{|\vec{s}_1 - \vec{s}_2|}, \qquad (1)$$

where Z_n designates the nuclear charge. The coordinates $\vec{s}_i$ $(i{=}1,2)$ are the Z_n-scaled coordinates $\vec{s}_i \equiv Z_n\vec{r}_i$ $(i = 1,2)$, where $\vec{r}_i$ is the position vector of the ith electron in the standard length unit with respect to the nucleus. In the standard Hamiltonian for the three-dimensional helium atom, $\vec{r}_i = (x_i, y_i, z_i)$, while in the present two-dimensional model, $\vec{r}_i = (x_i, y_i)$.

The Z_n-scaled coordinates $\vec{s}_i$ are of advantage over the standard coordinates $\vec{r}_i$ $(i = 1,2)$. For large Z_n values, the electron cloud is strongly compressed towards the nucleus due to the strong nuclear attraction potential. Therefore, the relevant length scale is very different from that associated with systems of small Z_n values. By multiplying $\vec{r}_i$ by Z_n so as to enlarge the length unit, the wave functions for different values of Z_n can be compared in the same length scale. Indeed, as shown by Eq. (1), the one-electron part of the Hamiltonian becomes independent of Z_n on condition that the energy is normalized by dividing it by Z_n^2. In this way, the effect of the electron-electron interaction becomes readily apparent.

The energies and wave functions corresponding to the solutions of the Schrödinger equation for the Hamiltonian (1) have been obtained by solving the full configuration interaction (FCI) matrix using a large $[20s10p7d]$ Gaussian basis set [23,24]. The probability density in the internal space, hereafter called the *internal probability density*, was extracted from the resultant FCI wave function $\Psi(\vec{s}_1, \vec{s}_2)$ by integrating over the angular coordinate ϕ_+ that is associated with an overall rotation.

Briefly, expressing the Cartesian coordinates (s_{xi}, s_{yi}) in terms of the polar coordinates (s_i, ϕ_i) $(i = 1,2)$ allows us to define two angular coordinates, namely, the ϕ_+ coordinate $\phi_+ = (\phi_1 + \phi_2)/2$ that is responsible for an overall rotation and is conjugate to the total orbital angular momentum, and the complementary ϕ_- coordinate $\phi_- = (\phi_1 - \phi_2)/2$. A set of three coordinates, $s_1 \equiv |\vec{s}_1|$, $s_2 \equiv |\vec{s}_2|$, and ϕ_-, defines then the internal space of the two-electron systems having circular symmetry. The probability density integrated over ϕ_+ and multiplied by the radial surface element $s_1 s_2$, namely, $|\Psi(s_1, s_2, \phi_-)|^2 s_1 s_2$, represents the internal probability density and is hereafter designated by ρ_{int}. The relationship between the internal angle ϕ_- and the commonly used *interelectronic angle* $\angle(e - \alpha - e)$, denoted by θ_{12}, is as follows. The individual polar angles ϕ_1 and ϕ_2, associated, respectively, with electrons 1 and 2, vary from 0 to 2π. Thus, the ϕ_- angle ranges between $-\pi$ and π. On the other hand, θ_{12} is defined as the interior angle of the triangle $e - \alpha - e$, with α as its vertex, and ranges between 0 and π. Consequently, some values of ϕ_- correspond to the same value of θ_{12} and we can write $\theta_{12} = 2|\phi_-|$ for $|\phi_-| \leqslant \pi/2$ and $\theta_{12} = 2(\pi - |\phi_-|)$ for $\pi/2 < |\phi_-| \leqslant \pi$. The computational procedure has been described in detail in our previous papers [23,24].

III. RESULTS AND DISCUSSION

A. Statistical and ground-state distributions

The probability-density distribution with respect to the two-electron angle ϕ_-, namely, the two-electron angular-density distribution $\sigma(\phi_-)$, has been obtained by integrating the internal probability density $\rho_{\text{int}}(s_1, s_2, \phi_-)$ over the two radial

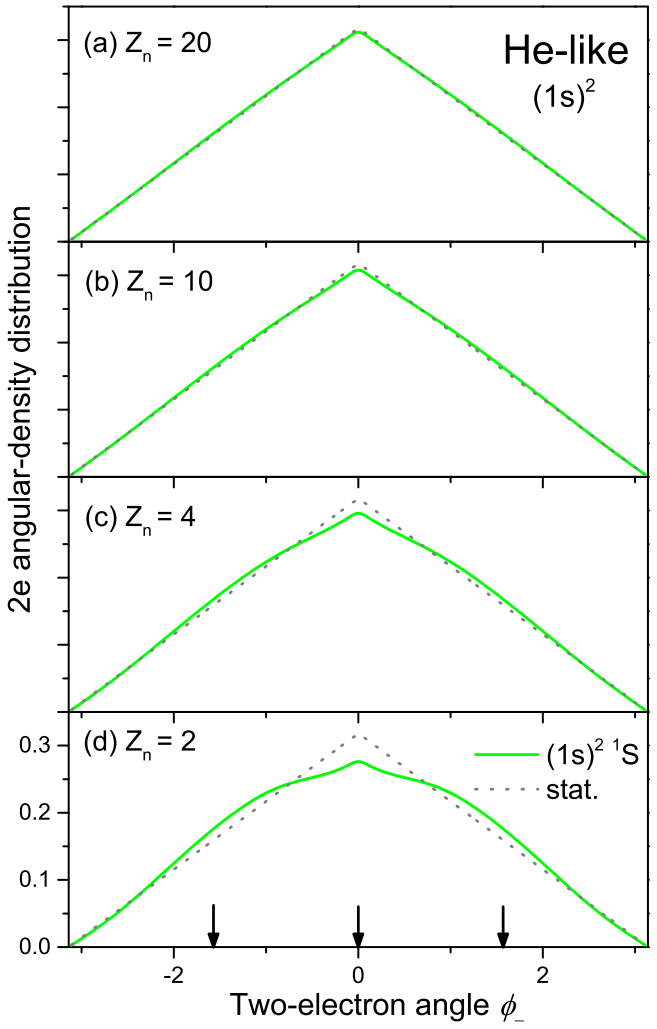

FIG. 1. (Color online) Two-electron angular-density distributions for the $(1s)^2$ ground state of He-like systems for different nuclear charge Z_n: (a)–(d) correspond, respectively, to the cases with $Z_n = 20$, 10, 4, and 2. The statistical distribution, defined by $(\pi - |\phi_-|)/\pi^2$, corresponding to the mutually independent rotation of the two electrons around the nucleus, is plotted as a dotted line in (a)–(d). The arrows in (d) indicate the special angles $\phi_- = 0$ and $\pm\pi/2$, which correspond, respectively, to the distinct spatial configurations of the two electrons where they align parallel on the same side of the nucleus and where they align antiparallel on opposite sides of the nucleus.

coordinates (s_1, s_2). The result for the $(1s)^2\ ^1S$ ground state together with the *statistical distribution* are displayed in Fig. 1. The statistical distribution, indicated in Fig. 1 by a dotted triangle, is given analytically by $(\pi - |\phi_-|)/\pi^2$ (cf. [23,24]). It reflects directly the volume element $2(\pi - |\phi_-|)$ for ϕ_+ which enters the internal probability density by the integration of $|\Psi(\vec{s}_1, \vec{s}_2)|^2$ over ϕ_+. The statistical triangle represents a special distribution in which the probability for the two electrons to take a particular value of the interelectronic angle θ_{12} is the same for all values of θ_{12}. This corresponds to the situation where both electrons vary their polar angles independently over the interval $[0, 2\pi]$, i.e., the two electrons rotate freely around the nucleus without correlation between them. This is confirmed by a simple geometrical analysis of the statistical triangular distribution since the set of internal angles $\pm\phi_-$ and $\pm(\pi - \phi_-)$ for $0 \leqslant \phi_- \leqslant \pi/2$ gives the same value of θ_{12}. Summing the probability distribution of Fig. 1 over the four internal angles gives the same value of $2/\pi$ for any θ_{12}.

There are two characteristic sets of angles for $\sigma(\phi_-)$, namely, $\phi_- = 0, \pm\pi$ and $\phi_- = \pm\pi/2$. The former set $\{0, \pm\pi\}$ is associated with a spatial configuration in which both electrons are located on the same side of the nucleus. On the other hand, the set of angles $\{\pm\pi/2\}$ corresponds to the situation where the electrons are on opposite sides of the nucleus. Thus, if an actual density distribution for some state has a larger value than the triangular statistical density at these angles, the electrons in such a state prefer to be on the same side of the nucleus for $\phi_- = 0, \pm\pi$ and on opposite sides of the nucleus for $\phi_- = \pm\pi/2$. These angles are indicated by arrows in Fig. 1(d). Since the density at $\phi_- = \pm\pi$ always vanishes because of the volume element $2(\pi - |\phi_-|)$, the angles $\phi_- = \pm\pi$ are not indicated by arrows in the figure.

The two-electron angular-density distributions for the $(1s)^2$ ground state displayed in Figs. 1(a)–1(d) show that for $Z_n = 20$, corresponding to the large Z_n regime, the density distribution closely follows the statistical distribution. This implies that in the regime of large Z_n, both electrons tend to move independently of one another around the nucleus. On the other hand, as Z_n decreases, the actual distribution deviates more and more strongly from the statistical distribution. Indeed, at $Z_n = 2$, corresponding to the helium atom, the density is significantly smaller than the statistical value at $\phi_- = 0$ and larger at $\phi_- = \pm\pi/2$. It indicates that the two electrons tend to be on mutually opposite sides of the nucleus and is consistent with recent results by Koga *et al.* [25,26].

This observation can be rationalized by considering the relative importance of the electron-electron interaction with respect to the one-electron component of the Hamiltonian as follows. In the regime of large Z_n, the role of the electron-electron interaction is very small relative to the one-electron component as implied by Eq. (1). Therefore, each of the two electrons can rotate freely around the nucleus. Their correlation is negligible even though both electrons occupy the same $(1s)$ orbital. With decreasing Z_n, however, the effect of the electron-electron interaction increases, forcing the electrons to be on opposite sides of the nucleus in order to avoid an energy increase due to the electron repulsion. The observed Z_n dependence for the ground state of He-like systems, i.e., *smaller* Z_n being associated with a larger angular correlation, is in accord with earlier studies for the doubly excited states [9,27]. In the next section, we shall see a counterintuitive trend for the singlet and triplet singly excited states of the $(1s)(2p)$ configuration, namely, a large angular correlation even for *larger* Z_n values.

B. Distributions for the $(1s)(2s)$ and $(1s)(2p)$ configurations

The two-electron angular-density distributions for the singlet-triplet pair of states of the $(1s)(2s)$ and $(1s)(2p)$ configurations for different Z_n values are displayed in Figs. 2 and 3, respectively. The results for the $(1s)(2s)$ configuration (Fig. 2) show that the density distribution closely follows the triangular statistical distribution, irrespective of the nuclear

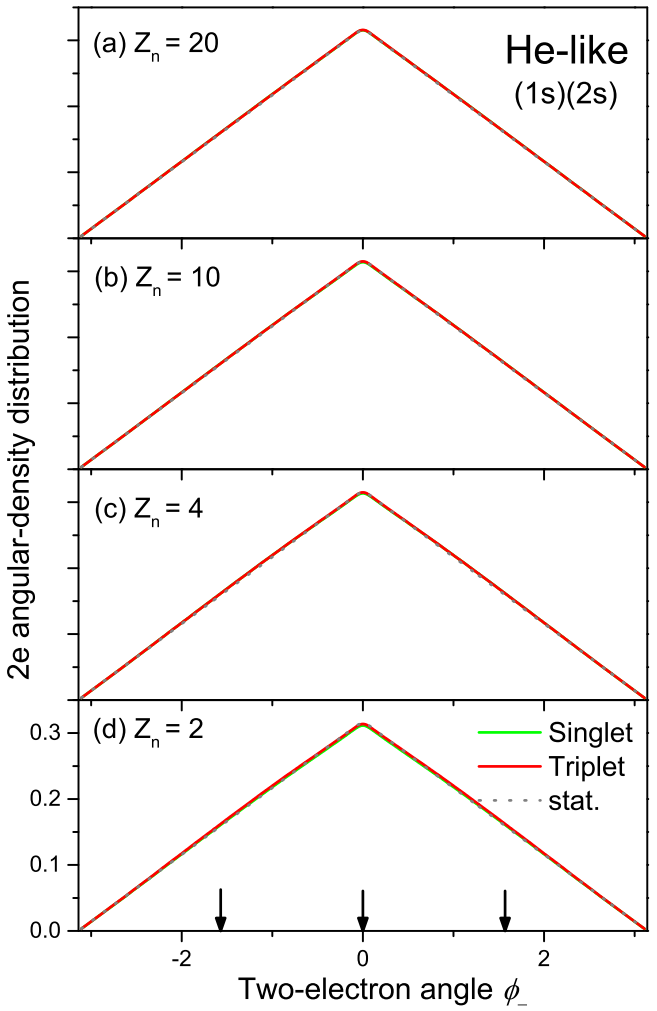

FIG. 2. (Color online) Two-electron angular-density distributions for the $(1s)(2s)$ singlet-triplet pair of states of He-like systems for different nuclear charge Z_n: (a)–(d) correspond, respectively, to the cases of $Z_n = 20$, 10, 4, and 2. The singlet and triplet distributions are displayed by green and red (light and dark gray), respectively. Both the singlet and the triplet distributions closely follow the statistical distribution for all Z_n values and thus could not be properly resolved on the scale used in the figure. See the caption to Fig. 1 for further details.

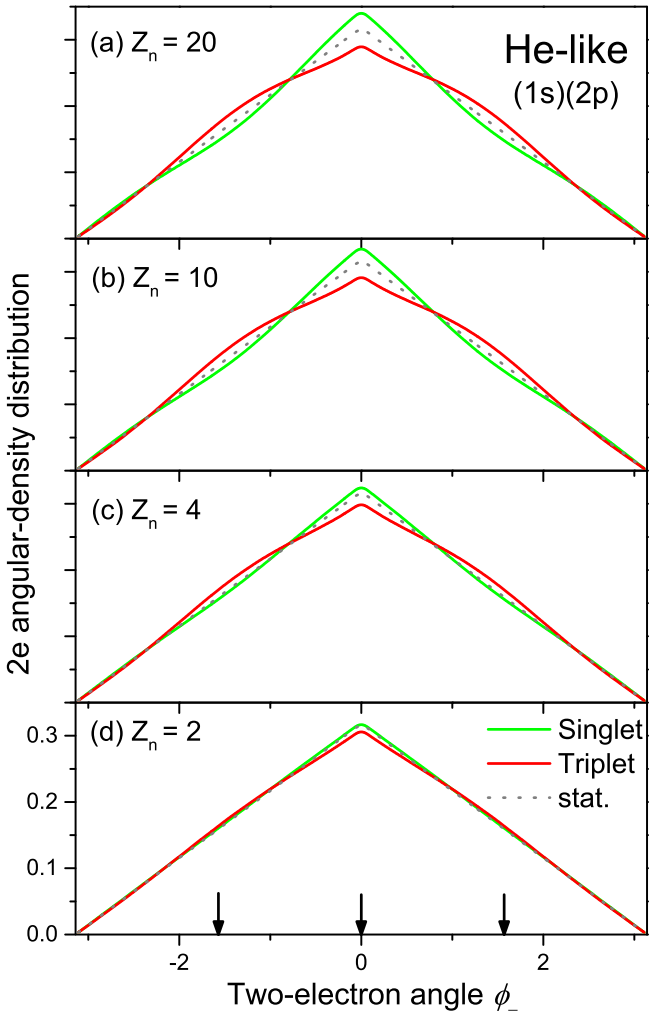

FIG. 3. (Color online) Two-electron angular-density distributions for the $(1s)(2p)$ singlet-triplet pair of states of He-like systems for different nuclear charge Z_n: (a)–(d) correspond, respectively, to the cases of $Z_n = 20$, 10, 4, and 2. The singlet and triplet distributions are displayed by green and red (light and dark gray), respectively. See the caption to Fig. 1 for further details.

charge Z_n for both the singlet $(1s)(2s)\ ^1S$ and the triplet $(1s)(2s)\ ^3S$ states. Therefore, the distribution of the two electrons around the nucleus in either the singlet or the triplet pair of states of the $(1s)(2s)$ configuration is only very weakly correlated.

The situation is different for the $(1s)(2p)$ singlet-triplet pair of states (Fig. 3). For small values of Z_n, such as $Z_n = 2$ [Fig. 3(d)], the two-electron angular-density distribution for both singlet and triplet states roughly follows the statistical triangle with only small deviations like in the $(1s)(2s)$ case. However, as Z_n increases, the distributions deviate more and more strongly from the statistical distribution. Further, the distribution of the singlet state has a larger density at $\phi_- = 0$ but a smaller density at $\phi_- = \pm\pi/2$ than the statistical distribution, while an opposite trend is observed for the triplet state. We recall that for increasing Z_n, the singlet and triplet wave functions approach those of the corresponding IPM based on the Hartree-Fock approximation as implied by Eq. (1), showing a decreasing role of the electron-electron interaction for increasing Z_n. Nonetheless, our results for the large Z_n regime indicate that the electrons in the singlet $(1s)(2p)\ ^1P$ state tend to be on the same side of the nucleus, while those in the triplet $(1s)(2p)\ ^3P$ state tend to be on the opposite sides of the nucleus. These results are consistent with those of the study by Thakkar *et al.* [13], who showed that the modulus of the angular correlation coefficients for the $(1s)(2s)$ pair of states is small irrespective of Z_n, while that for the $(1s)(2p)$ pair of states becomes increasingly larger for increasing Z_n, with mutually opposite signs between the singlet and the triplet states.

In the following section, we shall rationalize the observed trends by invoking the concepts of the *conjugate Fermi holes* as well as of the standard or *genuine* Fermi holes.

C. Structure of the genuine and conjugate Fermi holes in the internal space

In the limit of $Z_n \to \infty$, the orbital part of the two-electron wave functions for a pair of singlet and triplet states can be described exactly by single-determinant Hartree-Fock wave functions of the form

$$\Psi^+(\vec{s}_1,\vec{s}_2) = \frac{1}{\sqrt{2}}[\psi_a(\vec{s}_1)\psi_b(\vec{s}_2) + \psi_b(\vec{s}_1)\psi_a(\vec{s}_2)], \quad (2)$$

$$\Psi^-(\vec{s}_1,\vec{s}_2) = \frac{1}{\sqrt{2}}[\psi_a(\vec{s}_1)\psi_b(\vec{s}_2) - \psi_b(\vec{s}_1)\psi_a(\vec{s}_2)], \quad (3)$$

where the symmetric and antisymmetric functions, Ψ^+ and Ψ^-, are the singlet and triplet wave functions, respectively. The subscripts a and b may refer either to the $1s$ and $2s$ orbitals or to the $1s$ and $2p$ orbitals, respectively, in the case of the $(1s)(2s)$ or $(1s)(2p)$ singlet-triplet pair of states. Since these wave functions are *independent particle* wave functions, there is no correlation between the two electrons except for the well-known Fermi correlation in the *triplet* wave function, in which case the two electrons cannot occupy the same spatial position due to the fact that the antisymmetric triplet wave function vanishes at $\vec{s}_1 = \vec{s}_2$. On the other hand, as displayed in Fig. 3, we observe a strong angular correlation for the $(1s)(2p)$ pair of states in the regime of large Z_n, even for the *singlet* state. In contrast, we observe only weak correlation for the $(1s)(2s)$ pair in both the singlet and the triplet states.

In order to rationalize these trends, we focus particularly on the $(1s)(2p)$ singlet state showing a strong angular correlation for large Z_n and consider the difference in the probability-density distributions in the internal space between the singlet and the corresponding triplet states, i.e., the quantity $\rho^+_{\rm int}(s_1,s_2,\phi_-) - \rho^-_{\rm int}(s_1,s_2,\phi_-)$, in the limit of $Z_n \to \infty$. These values are displayed in Fig. 4(a) for the $(1s)(2s)$ configuration and in Fig. 4(b) for the $(1s)(2p)$ configuration. The three axes, X, Y, and Z, defining this internal space, correspond, respectively, to s_1, s_2, and ϕ_-. By definition, the domain for the angular coordinate ϕ_- is the interval $[-\pi,\pi]$, but the corresponding Z axis is labeled numerically in radians rather than in the units of π.

The blue and red (light and dark gray) surfaces in these figures represent, respectively, the regions where the singlet probability density is larger than the triplet density, and vice versa. In the limit of $Z_n \to \infty$, the blue regions represent the standard or genuine Fermi holes where the triplet state has a smaller density than the singlet state (cf. Fig. 4). In the internal space, these regions appear in the vicinity of the Z axis at $\vec{s}_1 = \vec{s}_2$. We note that the singlet and the triplet wave functions, as represented by Eqs. (2) and (3), give exactly the same electron density distribution as $|\psi_a(\vec{s})|^2 + |\psi_b(\vec{s})|^2$. Therefore, when there is a hole in the triplet wave function, namely, the Fermi hole, there must also be a hole somewhere in the corresponding singlet wave function in order for their electron densities to be balanced. The red regions displayed in Figs. 4(a) and 4(b) represent this hole in the singlet wave function and correspond to the so-called *conjugate Fermi holes* representing regions with a small density for the singlet state and a large density for the triplet states.

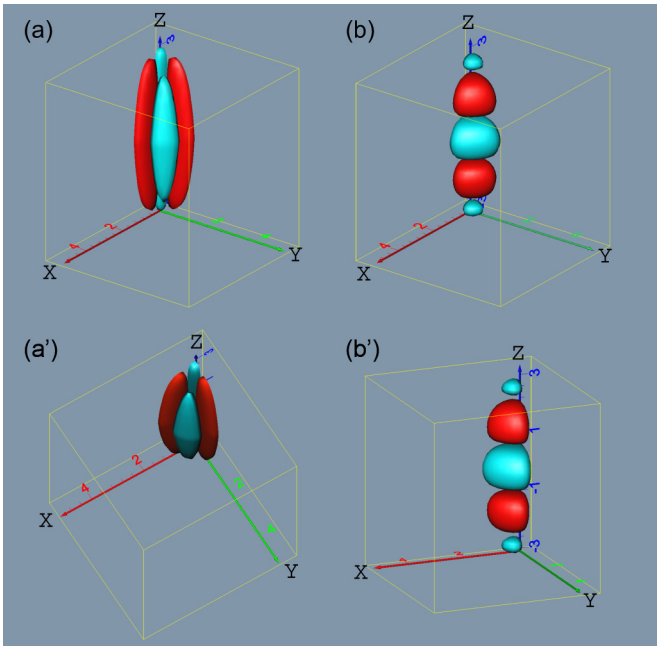

FIG. 4. (Color online) Difference in the probability-density distributions between the singlet-triplet pair of states of He-like systems in the limit of $Z_n \to \infty$. (a) The $(1s)(2s)$ configuration and (b) the $(1s)(2p)$ configuration. (a′) and (b′) represent the same distributions of (a) and (b), respectively, from a different viewpoint. The X, Y, and Z axes represent, respectively, the s_1, s_2, and ϕ_- coordinates (see the text). The square norm of the displayed surface is 0.005. The blue (light gray) and red (dark gray) surfaces correspond, respectively, to the regions where the probability density of the singlet wave function is larger than that of the triplet wave function (genuine Fermi hole), and vice versa (*conjugate Fermi hole*).

The mechanism that leads to the appearance of these conjugate Fermi holes has been explained in detail elsewhere [23,24] and is only briefly described here. There are two key conditions that are required for the appearance of conjugate Fermi holes. First, the two one-electron orbitals, ψ_a and ψ_b in Eqs. (2) and (3), must possess some spatially overlapping region since otherwise there would be no singlet-triplet difference in the probability densities as well as in the energy of these states. Second, one of the orbitals, ψ_a or ψ_b, has to have at least one node in this overlapping region. This second condition is automatically satisfied if ψ_a and ψ_b are orthogonal. Assuming that we choose coordinates $\vec{s}_1$ and $\vec{s}_2$ to be close to the nodal point $\vec{s}_0$ of, say, the orbital ψ_b, in such a way that this ψ_b orbital has opposite signs at $\vec{s}_1$ and $\vec{s}_2$, namely, that $\mathrm{sgn}[\psi_b(\vec{s}_1)\cdot\psi_b(\vec{s}_2)] = -1$, then the first and the second terms in the bracket on the right-hand side of the symmetric singlet wave function in Eq. (2) have different signs due to the change of the sign of ψ_b, thus canceling one another. On the other hand, in the case of the antisymmetric triplet wave function, the corresponding first and second term have equal signs since the sign change of the ψ_b orbital is canceled by the minus sign in front of the second term.

In the case of the $(1s)(2s)$ configuration, the $1s$ orbital has no node, while the $2s$ orbital has one node along the radial coordinate $s \equiv |\vec{s}|$. Due to the orthogonality between the $1s$ and $2s$ orbitals, this node of the $2s$ orbital is located in the range

of the s coordinate where the densities $|\psi_{1s}|^2$ and $|\psi_{2s}|^2$ have a nonzero overlap. Therefore, choosing two radial coordinates s_A and s_B so as to satisfy the condition $s_A < s_0 < s_B$, where s_0 is the location of the radial node of the $2s$ orbital, the first and the second terms on the right-hand side of Eq. (2) cancel one another, yielding the conjugate Fermi holes along the radial coordinates of s_1 and s_2 as displayed in Fig. 4(a). In the case of the $(1s)(2p)$ configuration, on the other hand, the $2p$ orbital has no radial node but an angular node. The ψ_{2p} orbital changes its phase at $\phi = \pi$ when its angular coordinate ϕ varies over the interval $[0,2\pi]$. Therefore, recalling the factor 2 in the definition of the internal ϕ_- angle, i.e., $\phi_- = (\phi_1 - \phi_2)/2$, the wave function Ψ^+ of Eq. (2) has two conjugate Fermi holes located along the angular Z axis at $\phi_- = \pm\pi/2$, as is apparent from Fig. 4(b).

D. Interpretation

The observed trend of the ϕ_- dependence of the probability-density distribution (cf. Figs. 2 and 3), i.e., the strong dependence for the $(1s)(2p)$ singlet-triplet pair of states in the large Z_n regime and the very weak dependence for the $(1s)(2s)$ pair of states for all Z_n values, can be rationalized by using the concept of the genuine and conjugate Fermi holes, as outlined in the preceding section. For this purpose, we have computed the difference in the probability density between the $(1s)(2s)$ singlet-triplet pair of states and between the $(1s)(2p)$ pair of states for the nuclear charges $Z_n = 20$, 10, 4, and 2, displayed in Figs. 5 and 6, respectively. In these figures, we also plotted the electron-electron interaction potential of the scaled Hamiltonian, i.e., the third term on the right-hand side of Eq. (1), as an isoenergy surface for the corresponding values of Z_n. As displayed in these figures, the electron-electron interaction potential manifests itself in the internal space as three striking "poles" peaked at $\phi_- = 0, \pm\pi$. Since the electron-electron repulsion is very strong around these poles, the probability densities of both singlet and triplet states tend to avoid the regions in the vicinity of these poles.

For the large nuclear charge $Z_n = 20$, the structure of the blue and red (light and dark gray) surfaces for the $(1s)(2s)$ configuration and for the $(1s)(2p)$ configuration [Figs. 5(a) and 6(a)] is similar to that of the corresponding genuine and conjugate Fermi holes displayed in Figs. 4(a) and 4(b), respectively. This similarity is due to the fact that in this large Z_n regime, the electron-electron interaction is very weak, as confirmed by the isoenergy surface of Figs. 5(a′) and 6(a′). Therefore, the wave functions of the singlet and triplet states are close to those of the independent particle model of Eqs. (2) and (3).

In the case of the $(1s)(2s)$ configuration, the genuine and conjugate Fermi holes are located along the X and Y axes representing the radial s_1 and s_2 coordinates, and no structure is observed along the Z axis representing the angular ϕ_- coordinate. This is due to the fact that the ψ_{2s} orbital that is responsible for the appearance of conjugate Fermi holes has a radial node instead of an angular node. This is also confirmed by the fact that in the $Z_n \to \infty$ limit, the singlet and triplet wave functions for the $(1s)(2s)$ configuration do not depend on angular variables since the $1s$ and $2s$ orbitals have zero angular momentum. Therefore, the two-electron

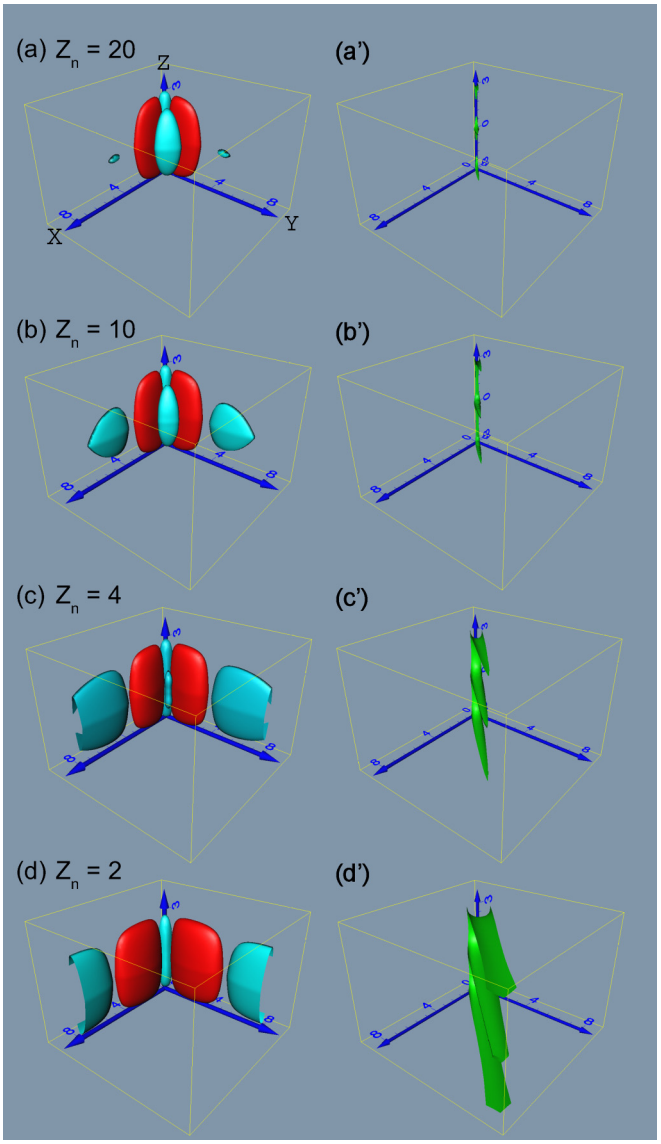

FIG. 5. (Color online) Difference in the probability-density distributions between the $(1s)(2s)$ ^1S singlet state and the $(1s)(2s)$ ^3S triplet state of He-like systems in the internal space: (a)–(d) correspond, respectively, to the cases with $Z_n = 20$, 10, 4, and 2. The X, Y, and Z axes represent, respectively, the s_1, s_2, and ϕ_- coordinates. The square norm of the displayed surface is 0.001. The blue (light gray) and red (dark gray) surfaces correspond, respectively, to regions in which the probability density of the singlet wave function is larger than that of the triplet wave function, and vice versa. Figures (a′)–(d′) indicate the Z_n-adjusted electron repulsion potential [cf. Eq. (1)] for the corresponding cases. The displayed surfaces represent the area where the electron repulsion potential energy becomes larger than 0.5 a.u.

angular density distributions for the $(1s)(2s)$ pair of states for large Z_n, such as $Z_n = 20$, closely follow the statistical distribution as observed in Fig. 2(a). As Z_n decreases, the poles of the electron-electron interaction potential become stronger, as shown in Figs. 5(a′)–5(d′), and affect the probability-density distributions of the $(1s)(2s)$ pair of states. Indeed, the singlet probability density associated with the blue (light gray) surface located around $\phi_- = 0$ in Fig. 5(a) decreases significantly with

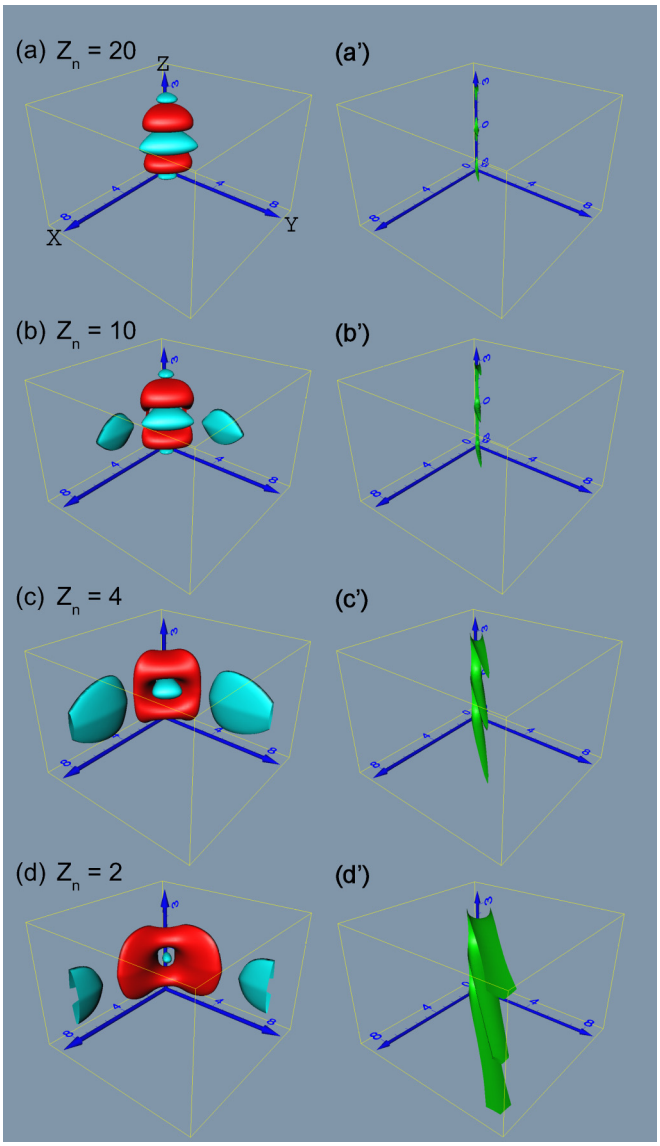

FIG. 6. (Color online) Difference in the probability-density distributions between the $(1s)(2p)\ ^1P$ singlet state and the $(1s)(2p)\ ^3P$ triplet state of He-like systems in the internal space: (a)–(d) correspond, respectively, to the cases with $Z_n = 20$, 10, 4, and 2. See caption to Fig. 5 for further details.

decreasing Z_n [Figs. 5(b)–5(d)] due to the strong potential pole of the electron-electron interaction. The singlet probability density that migrated from this region is now located, however, in regions with larger s_1 or s_2 but at almost the same value of ϕ_-. Due to the zero angular momentum of the $1s$ and $2s$ electrons, they avoid the strong potential pole by simply increasing the interelectron distance while hardly changing their angle. This is the reason why the two-electron angular-density distributions of the singlet-triplet pair of states for the $(1s)(2s)$ configuration depend only very weakly on ϕ_-, even for small Z_n where the electron-electron interaction is strong.

In contrast to the $(1s)(2s)$ case, the genuine and conjugate Fermi holes that are associated with the $(1s)(2p)$ configuration are located along the Z axis (representing the angular coordinate ϕ_-) showing an angular alignment of these holes. Further, an inspection of Fig. 4(b) shows that the genuine Fermi holes are, in this case, located at $\phi_- = 0, \pm\pi$, whereas the conjugate Fermi holes are located at $\phi_- = \pm\pi/2$. Recalling that the triplet density is smaller than the singlet density in genuine Fermi holes and larger than the singlet density in conjugate Fermi holes, we see that the observed ϕ_- dependence of the two-electron angular-density distribution for the $(1s)(2p)$ triplet state is in accord with the existence of the genuine and conjugate Fermi holes. Similarly, since the singlet probability density is smaller and larger than the triplet probability in the conjugate and in the genuine Fermi holes, respectively, the two-electron angular-density distribution for the $(1s)(2p)$ singlet state shows smaller and larger densities at the location of the conjugate and genuine Fermi holes, respectively. These coincidences indicate that the observed strong ϕ_- dependence of the probability-density distributions for the $(1s)(2p)$ singlet-triplet pair of states in the large Z_n regime can be rationalized by the appearance of the genuine and conjugate Fermi holes due to the decreasing electron-electron interaction.

As the nuclear charge Z_n decreases, the electron-electron interaction becomes stronger, as displayed in Figs. 6(a′)–6(d′). It is noted that by definition, the genuine Fermi holes exist in the vicinity of the regions satisfying $\vec{s}_1 = \vec{s}_2$. The electron-electron interaction potential $\frac{1}{Z_n}\frac{1}{|\vec{s}_1 - \vec{s}_2|}$ diverges to infinity in the same region. Consequently, the three "poles" of the electron-electron interaction penetrate exactly into the three blue surfaces of the genuine Fermi holes, as displayed in Fig. 4(b). As Z_n decreases, the singlet probability density located in these genuine Fermi holes is forced by the strong poles of the electron-electron interaction to migrate away from the Z axis, as displayed in Figs. 6(b)–6(d). Since, unlike the $2s$ electron, the $2p$ electron has a nonzero angular momentum, the singlet probability density that migrates from the Fermi holes is located in regions with different values of ϕ_-. This levels out the probability density along the ϕ_- axis and explains the observed weak ϕ_- dependence of the probability density for the small nuclear charge $Z_n = 2$.

IV. SUMMARY

In the present study, the angular correlation in the ground and singly excited states of the two-dimensional He and He-like atomic ions has been studied by relying on highly accurate full configuration interaction (FCI) wave functions. The two-electron angular-density distributions have been calculated by integrating the square modulus of the FCI wave functions over all coordinates other than the two-electron angle ϕ_- defined by the difference between the two polar angles ϕ_1 and ϕ_2 for the respective electrons 1 and 2.

The resultant distribution for the $(1s)^2$ ground state in the regime of large nuclear charges Z_n shows a very weak ϕ_- dependence, while the dependence increases for small Z_n values, such as for $Z_n = 2$ of the helium atom. This dependence is in accord with the variation of the electron correlation in units of the Z_n-adjusted correlation energy $\frac{\Delta E_{\rm corr}}{Z_n^2}$. In contrast, the two-electron angular density distributions for the singly excited states of the $(1s)(2s)$ and $(1s)(2p)$ configurations have a different character than those for the $(1s)^2$ ground state: In the case of the $(1s)(2s)$ configuration, the singlet and the triplet

states show only a very weak dependence on ϕ_- irrespective of Z_n, while in the case of the $(1s)(2p)$ configuration, both the singlet and the triplet states show a *weak* dependence for *small* Z_n yet a *strong* dependence for *large* Z_n, in spite of the fact that the electron correlation decreases towards zero for increasing Z_n. Further, in the large Z_n regime, the singlet state of the $(1s)(2p)$ configuration shows a peak in probability density at $\phi_- = 0$, indicating a tendency of the two electrons to be on the same side of the nucleus. On the other hand, in the case of the corresponding triplet state, the probability density is peaked at $\phi_- = \pm\pi/2$, indicating a tendency of the two electrons to be on opposite sides of the nucleus. We would like to emphasize that this counterintuitive trend that we find for the $(1s)(2p)$ configuration is not limited to the present 2D model. Thakkar and Smith have already identified a similar behavior for the same states in their evaluation of the angular correlation coefficients for regular 3D He-like systems [13].

In order to rationalize the observed trends of the angular ϕ_- dependence of the probability density, focusing particularly on the unexpected trend found for the $(1s)(2p)$ singlet-triplet pair of states with respect to the variation of Z_n, we have examined in detail the probability-density distributions of the relevant states in the *internal space* defined by the Z_n-adjusted radial coordinates s_i $(i = 1,2)$ and the two-electron angle ϕ_-. The difference in the probability densities between the singlet-triplet pair of states in the internal space in the $Z_n \to \infty$ limit defines, respectively, the genuine and the *conjugate* Fermi holes in which the singlet probability density is larger than the triplet density, and vice versa. The genuine and conjugate Fermi holes for the $(1s)(2s)$ singlet-triplet pair show no structure along the angular ϕ_- coordinate. This is consistent with the two-electron angular-density distributions for the $(1s)(2s)$ pair of states showing a very weak ϕ_- dependence irrespective of the nuclear charge Z_n. In contrast, the genuine and conjugate Fermi holes for the $(1s)(2p)$ singlet-triplet pair of states align alternately along the ϕ_- axis. They are centered at $\phi_- = 0,\pm\pi$ for the genuine Fermi holes and at $\phi_- = \pm\pi/2$ for the conjugate Fermi holes. Since the triplet density is smaller than the singlet density in genuine Fermi holes and larger than the singlet density in conjugate Fermi holes, the observed strong ϕ_- dependence for the $(1s)(2p)$ singlet-triplet pair of states in the large Z_n regime is supported by the appearance of these holes due to the decreasing electron-electron interaction for increasing Z_n.

Recent advances in high-power free-electron lasers for extreme ultraviolet (EUV) and x-ray wavelength regions have enabled us to study nonlinear multiphoton processes in simple atoms [28,29]. We note that these pioneering experiments have succeeded in generating Rabi oscillations between the $(1s)^2$ ground state and the $(1s)(2p)$ singlet state in the helium atom [30], indicating a possibility of transferring the whole probability density from the ground state to the $(1s)(2p)$ excited state at a certain time. Combining it with the $(e,2e)$ type of experiments [31] that measure the correlated two electrons instantaneously ejected from the target atom, it should be feasible to design an ambitious experiment which would enable one to directly observe the anisotropic distribution of the two electrons that have been explored in the present study. This would thus experimentally verify the existence of the conjugate Fermi holes as well as of the standard Fermi holes.

ACKNOWLEDGMENTS

The present study has been supported in part by the Grants-in-Aid for Scientific Research (C) (No. 23550025) and the Grants-in-Aid for Scientific Research on Innovative Areas (No. 25110006) of the Japan Society for the Promotion of Science (JSPS), and by the Nihon University Strategic Projects for Academic Research. T.S. and J.P. would like to thank the Alexander von Humboldt Foundation for its kind support and Geerd H. F. Diercksen and the Max-Planck-Institute for Astrophysics in Garching for their hospitality.

[1] R. P. Madden and K. Codling, Astrophys. J. **141**, 364 (1965).
[2] M. E. Rudd, Phys. Rev. Lett. **15**, 580 (1965).
[3] D. R. Herrick and M. E. Kellman, Phys. Rev. A **21**, 418 (1980).
[4] D. R. Herrick, M. E. Kellman, and R. D. Poliak, Phys. Rev. A **22**, 1517 (1980).
[5] M. E. Kellman and D. R. Herrick, Phys. Rev. A **22**, 1536 (1980).
[6] P. Rehmus, C. C. J. Roothaan, and R. S. Berry, Chem. Phys. Lett. **58**, 321 (1978).
[7] P. Rehmus, M. E. Kellman, and R. S. Berry, Chem. Phys. **31**, 239 (1978).
[8] H.-J. Yuh, G. Ezra, P. Rehmus, and R. S. Berry, Phys. Rev. Lett. **47**, 497 (1981).
[9] G. S. Ezra and R. S. Berry, Phys. Rev. A **28**, 1974 (1983).
[10] E. R. Davidson, J. Chem. Phys. **41**, 656 (1964).
[11] E. R. Davidson, J. Chem. Phys. **42**, 4199 (1965).
[12] N. Moiseyev and J. Katriel, Chem. Phys. **10**, 67 (1975).
[13] A. J. Thakkar and V. H. Smith, Jr., Phys. Rev. A **23**, 473 (1981).
[14] P. E. Regier and A. J. Thakkar, J. Phys. B **17**, 3391 (1984).
[15] J. M. Ugalde and R. J. Boyd, Chem. Phys. Lett. **114**, 197 (1985).
[16] J. M. Ugalde, R. J. Boyd, and J. S. Perkyns, J. Chem. Phys. **87**, 1216 (1987).
[17] N. M. Cann, R. J. Boyd, and A. J. Thakkar, J. Chem. Phys. **98**, 7132 (1993).
[18] J. Katriel and R. Pauncz, Adv. Quantum Chem. **10**, 143 (1977).
[19] R. J. Boyd, Nature (London) **310**, 480 (1984).
[20] Y. Sajeev, M. Sindelka, and N. Moiseyev, J. Chem. Phys. **128**, 061101 (2008).
[21] T. Sako, J. Paldus, and G. H. F. Diercksen, Phys. Rev. A **81**, 022501 (2010).
[22] T. Oyamada, K. Hongo, Y. Kawazoe, and H. Yasuhara, J. Chem. Phys. **133**, 164113 (2010).
[23] T. Sako, J. Paldus, A. Ichimura, and G. H. F. Diercksen, Phys. Rev. A **83**, 032511 (2011).
[24] T. Sako, J. Paldus, A. Ichimura, and G. H. F. Diercksen, J. Phys. B: At. Mol. Opt. Phys. **45**, 235001 (2012).
[25] T. Koga and H. Matsuyama, Chem. Phys. Lett. **375**, 565 (2003).
[26] T. Koga, H. Matsuyama, and A. J. Thakkar, Chem. Phys. Lett. **512**, 287 (2011).
[27] P. C. Ojha and R. S. Berry, Phys. Rev. A **36**, 1575 (1987).

[28] Y. Hikosaka, M. Fushitani, A. Matsuda, C.-M. Tseng, A. Hishikawa, E. Shigemasa, M. Nagasono, K. Tono, T. Togashi, H. Ohashi *et al.*, Phys. Rev. Lett. **105**, 133001 (2010).

[29] N. Miyauchi, J. Adachi, A. Yagishita, T. Sako, F. Koike, T. Sato, A. Iwasaki, T. Okino, K. Yamanouchi, K. Midorikawa *et al.*, J. Phys. B: At. Mol. Opt. Phys. **44**, 071001 (2011).

[30] T. Sako, J. Adachi, A. Yagishita, M. Yabashi, T. Tanaka, M. Nagasono, and T. Ishikawa, Phys. Rev. A **84**, 053419 (2011).

[31] E. Weigold and I. E. McCarthy, *Electron Momentum Spectroscopy* (Kluwer Academic/Plenum, New York, 1999).